

A general approach using spiroborate reversible cross-linked Au nanoparticles for visual high-throughput screening of chiral vicinal diols†

Cite this: *Chem. Sci.*, 2013, **4**, 1156

Weili Wei, Li Wu, Can Xu, Jinsong Ren and Xiaogang Qu*

Since enantiopure vicinal diols are important intermediates for the synthesis of numerous pharmaceutical and industrial products, enantioseparation of chiral vicinal diols has received much attention. Here we report a stepwise protocol for creating high-throughput screening (HTS) assays for concentration and enantiomeric excess (ee) of vicinal diols applied to asymmetric dihydroxylation (AD) reactions by using spiroborate reversible cross-linked Au nanoparticles (AuNPs). The enantioselective assays have been demonstrated by NMR spectroscopy and successfully used to rapidly analyze the AD reactions of *trans*-stilbene with different reaction time and chiral ligands. The first and second steps involve the decoration of a small library of chiral AuNPs with saccharides that possess chiral *cis*-vicinal diol sites, and verification of the borate-directed assembly and disassembly of the chiral AuNPs. The third step concerns discovery of the optimal chiral AuNPs for a given analyte. The fourth step involves the evaluation of the accuracy and HTS performance of the method. The errors resulting from the analysis of true unknowns are remarkably low, within 2.7% for ee and 0.05 mM for total concentration. The method developed for hydrobenzoin has been applied to analyze the real AD reactions of *trans*-stilbene. Since the enantioseparation is based on enantioselective ligand exchange (eLE) principle and the reversibility of boron chemistry, this proof of concept approach can be easily adapted to other kinds of asymmetric reactions by using relevant optical nanoprobes.

Received 21st September 2012
Accepted 19th December 2012

DOI: 10.1039/c2sc21571c

www.rsc.org/chemicalscience

Introduction

The unique reversible properties of boron have attracted great interest in the field of dynamic-covalent chemistry.¹ Both boronic acids and the borate ion ($\text{B}(\text{OH})_4^-$) are versatile building blocks for reversible assembly. The use of the borate ion is particularly appealing because one borate can bind two *cis*-vicinal diols forming a spiroborate diester with dynamic-covalent behavior under certain conditions or under action of certain external chemical stimulus.^{1,2} This has promoted the production of a wide range of borate molecular devices, such as membrane transport carriers,³ chromatography solid supports,⁴ and chemosensors.⁵ Cross-linking reactions between borate ions and the *cis*-diol sites on polysaccharide chains has also been utilized to prepare polysaccharide-based reversible gels.⁶ Most recently, evidence suggests that borate even functions in the primary cell walls of plants, where it cross-links the pectic polysaccharide rhamnolacturonan II (RG-II) by forming spiroborate diesters.⁷

While progress in this research area has been rapid, the use of spiroborate for the construction of nanomaterial-based assemblies is still scarce,⁸ particularly those with capability of chiral recognition has not been reported yet.

Among various nanomaterials, gold nanoparticles (AuNPs) have been touted to be promising and useful in many applications because of their distinctive physical and optical properties. In particular, the plasmon resonance band of AuNPs can be changed by modulating the distance between AuNPs along with the color change of the AuNP solution.⁹ Reaction of borate ions with AuNPs that contain *cis*-vicinal diols on their surface could lead to AuNP networks that are composed of covalent, yet readily reversible spiroborate diester linkages. The dynamic-covalent nature of the spiroborate cross-links would allow the AuNP networks to reconfigure their assembly structures in the presence of external chemical stimulus such as *cis*-vicinal diols that compete for bonding with the borate.^{1,2c} That is, the spiroborate linkages between the AuNPs can be induced to dissociate *via* the competitive reaction of diols with the central borate. As a consequence, the resulting variation of the distances among AuNPs would allow the translation of the weak molecular interaction events into color changes, which can be monitored by commonly used instruments such as a UV-vis spectrometer or even the naked eye.

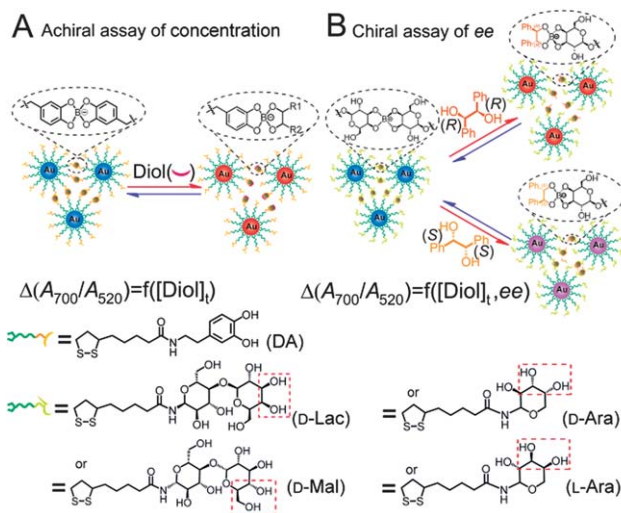
Laboratory of Chemical Biology, Division of Biological Inorganic Chemistry, State Key Laboratory of Rare Earth Resource Utilization, Changchun Institute of Applied Chemistry, Chinese Academy of Sciences, Changchun, 130022, P. R. China. E-mail: xqu@ciac.jl.cn; Fax: +86 431-85262625

† Electronic supplementary information (ESI) available. See DOI: 10.1039/c2sc21571c

To further develop the spiroborate reversible cross-linked AuNP assemblies, we endowed them with a chiral selective responding capability through an enantioselective ligand exchange (eLE) process.¹⁰ The process involves a competitive binding event, between two chiral ligands (defined as chiral selector and chiral analyte), to a center ion (Scheme S1, ESI[†]). This has allowed successful enantioseparation of chiral vicinal diols in capillary electrophoresis (CE) by using the borate as the center ion.¹⁰ As proved by both experimental and computational results,^{10,11} the eLE process relies on the energetic difference of the two diastereometric ternary spiroborates that are composed of chiral selector-borate-enantiomer of the analyte (suppose the analyte has two enantiomers). Similarly, by decorating AuNPs with chiral diols, the external chiral diol (analyte) triggered dissociation of the spiroborate cross-links between the AuNPs should also undergo the eLE process. This means different enantiomers of the same chiral diol analyte would induce a different reconfiguration of the AuNPs assemblies as well as a different color change of the solution. Consequently, these thoughts have motivated us to design a general approach for applying spiroborate cross-linked AuNPs to a high-throughput screening (HTS) assay of both enantiomeric excess (*ee*) and total concentration ($[\text{Diol}]_t$) of chiral vicinal diols, which has not been reported.

Chiral vicinal diols are important intermediates in the synthesis of numerous pharmaceuticals and industrial products such as chiral drugs, pesticides, liquid crystal materials, and fine chemicals.¹² They can be produced from olefins through the well-known asymmetric dihydroxylation (AD) reactions.¹³ To date, the ever-increasing demand for enantiopure vicinal diols has been accompanied by progress in the design of catalytic AD systems and combinatorial methods that can obtain large numbers of enantiopure products in a short time. However, monitoring of asymmetric chemical transformations, including *ee* and $[\text{Diol}]_t$ determination, remains the main bottleneck in these processes because it usually entails laborious and time-consuming chromatographic techniques¹⁰ or sophisticated instrument-demanded chiral nuclear magnetic resonance (NMR) spectroscopy.¹⁴ Therefore, development of spiroborate cross-linked AuNP assemblies for colorimetric visual HTS assay of both *ee* and $[\text{Diol}]_t$ of general chiral vicinal diols is of great importance.

To realize our strategy, AuNPs were decorated with thioctic amides terminated in an achiral vicinal diol dopamine (DA) or chiral saccharides including *D*-lactose (*D*-Lac), *D*-maltose (*D*-Mal), *D*-arabinose (*D*-Ara), and *L*-arabinose (*L*-Ara) and cross-linked with borate ions by forming dynamic-covalent spiroborates between the *cis*-vicinal diol sites under alkaline conditions (Scheme 1).^{14,15} The AuNPs are cross-linked by multiple spiroborate linkages and their gold cores are kept separate by the sufficient steric stabilization of the cyclic disulfide anchoring of thioctic amides allowing reversible assembly.¹⁶ For the achiral DA-AuNPs assemblies, they could be dissociated by vicinal diol analytes independent of chirality and the resulting blue shift of the plasmon resonance band of the AuNPs allows the determination of total concentration of both enantiomers ($[\text{Diol}]_t$, Scheme 1A). On the other hand, assemblies of the chiral AuNPs,



Scheme 1 Proposed mechanism for the AuNPs-based determination of $[\text{Diol}]_t$ and *ee* of chiral vicinal diols (appropriate to the work described herein for hydrobenzoin), and the molecular structures of achiral and chiral modifiers. $\Delta(A_{700}/A_{520})$, change of absorbance ratios caused by the shift of AuNPs's plasmon resonance band; $[\text{Diol}]_t$, total vicinal diol concentration; *ee*, enantiomeric excess. The red frames indicate the *cis*-vicinal diol sites.¹⁵

including *D*-Lac-AuNPs, *D*-Mal-AuNPs, *D*-Ara-AuNPs and *L*-Ara-AuNPs, allow us to quantify *ee* in addition to $[\text{Diol}]_t$ through the eLE process (Scheme 1B). We use *D*-Lac, *D*-Mal, *D*-Ara and *L*-Ara as chiral modifiers of the AuNPs because they are naturally chiral, readily available, and enantioselectivity of their terminal residues (*D*-galactose, *D*-glucose, *D*-arabinose, and *L*-arabinose, respectively) to chiral vicinal diols has been confirmed in eLE-CE.^{10b,c} Moreover, reversible cross-linking of saccharides *via* spiroborate has been well explored in both artificial molecular devices^{3–6} and natural plant biology.⁷ Therefore, HTS assay of both $[\text{Diol}]_t$ and *ee* could be achieved by batch monitoring the color changes with a 96-well plate analysis system. Compared to the previously reported chemosensor using enantiopure boronic acid as chiral selector,¹⁷ this AuNPs-based strategy have certain advantages such as ready availability of chiral reagents (the natural saccharides) and more distinct color changes which span a wider range from red to blue. As a result, an instant pre-screening of both $[\text{Diol}]_t$ and *ee* by direct use of the naked eye could be realized.

Results and discussion

A small library of chiral saccharide-decorated AuNPs (*D*-Lac-AuNPs, *D*-Mal-AuNPs, *D*-Ara-AuNPs and *L*-Ara-AuNPs) were prepared because different chiral analytes will not be best enantioselectively discriminated by one single chiral selector. Therefore, we anticipated that it would be advantageous to screen each new analyte (chiral diols) with the library of chiral AuNPs.

Our first goal was to prove the assembly of the modified AuNPs with borate ions. As an example of the investigations, spiroborate cross-linked assembly of *D*-Lac-AuNPs containing surface-bound *D*-Lac (0.04 mM) was complete at a molar ratio of

borate ion to the surface-bound *D*-Lac = 1 : 2 equiv. (Fig. S1, ESI[†]). This was in accordance with the stoichiometric ratio of the borate ion to *D*-Lac for forming spiroborate diesters (as cross-linkers) and the previously reported results.^{2b} Thus the optimal molar ratio of borate ions to the surface-bound *D*-Lac (1 : 2 equiv.) was used in all subsequent procedures. Time-dependent experiments (Fig. 1A) showed that the borate ion-directed assembly of *D*-Lac-AuNPs clusters took place as a rapid red-shift of plasmon resonance band in the first 2 min, and then reached equilibrium over the next 3 min. In the presence of 0.02 mM borate ions, the characteristic assembly time (τ_{asm}) of *D*-Lac-AuNPs was about 3 min (Fig. S2, ESI[†]), which was in accordance with the time scale of the reaction rate of forming borate esters.¹⁸ The results indicated that the borate-directed assembly was fast. Both dynamic light scattering (DLS) and transmission electron microscopy (TEM) experiments further confirmed that borate could induce *D*-Lac-AuNPs aggregation (Fig. 1B–D). In a similar way, the borate-directed assembly of other AuNPs (*D*-Mal-AuNPs, *D*-Ara-AuNPs, *L*-Ara-AuNPs, and DA-AuNPs) was obtained at 1 : 2 equiv. of borate ion to each bound diol (*D*-Mal, *D*-Ara, *L*-Ara, and DA) (Fig. S3A, ESI[†]). In addition, control experiments indicated that the UV-vis spectra of *D*-Lac-AuNPs were not affected by other common ions (Fig. S3B, ESI[†]) and amino or thiol group containing small molecules (Fig. S3C, ESI[†]), and UV-vis spectra of thioctic acid modified AuNPs were independent of borate ion (data not shown).

Next, we tested disassembly of the AuNPs clusters in the presence of diol analytes. Fig. 1D showed characteristic TEM images of the *D*-Lac-AuNPs assemblies which were disassembled upon incubation with a vicinal diol hydrobenzoin (1.0 mM) for 10 min (Fig. 1E). The UV-vis spectrum of the *D*-Lac-AuNPs solution was blue-shifted, as expected following the dissociation of the assemblies (Fig. S4, ESI[†]).

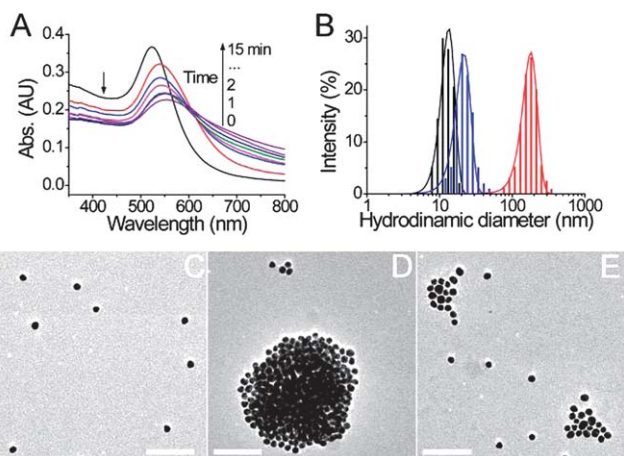


Fig. 1 (A) Variation in the UV-vis spectra of *D*-Lac-AuNPs (containing surface-bound *D*-Lac 0.04 mM) with time after the addition of borate ion at a concentration of 0.02 mM. The measurements were carried out in water solutions containing 20 vol% methanol (pH 9.5). (B) Size distribution of the particles as determined by DLS for *D*-Lac-AuNPs (black), *D*-Lac-AuNPs in the presence of borate ion (red), and *D*-Lac-AuNPs in the presence of borate ion and diol (blue); (C) TEM images of *D*-Lac-AuNPs; TEM images of the assembly (D) and disassembly (E) of *D*-Lac-AuNPs. Scale bar: 100 nm.

With the above results, enantioselective disassembly of the chiral AuNPs clusters with a chiral analyte (hydrobenzoin as a model) was further investigated. Since the aggregation of AuNPs generally resulted in a significant increase in the absorbance at 700 nm (A_{700}) and decrease in the absorbance at 520 nm (A_{520}), the ratio of A_{700} to A_{520} (A_{700}/A_{520}) was chosen to reflect the assembly of AuNPs.¹⁹ A higher ratio corresponded to assembled clusters of AuNPs with blue color whereas a lower ratio referred to dispersed AuNPs with red color. Thus a representative enantiodisassembly of the *D*-Lac-AuNPs aggregates with (*R,R*- and (*S,S*)-hydrobenzoin was shown in Fig. 2. As expected, the A_{700}/A_{520} values decreased enantiodifferently for the two enantiomers. The enantioselective disassembly of the other designed chiral AuNPs with the two enantiomers of hydrobenzoin were also observed (Fig. S5–S7, ESI[†]).

After succeeding in the test of enantioselective disassembly, we intended to screen out which chiral AuNPs could have the best discrimination between the two enantiomers for the model diol analyte (hydrobenzoin). Traditionally, acquiring this information would require time-consuming measurements of various UV-vis spectra as described above. For the purpose of HTS, the screening was performed with a 96-well plate analysis system. A “screening plate” was generated with chiral AuNPs (*D*-Lac-AuNPs, *D*-Mal-AuNPs, *D*-Ara-AuNPs, and *L*-Ara-AuNPs) and the optimum ratio (1 : 2 equiv.) of each AuNP with a borate ion was added to each well of the plate (Fig. 3A).

Previous studies^{17,20} indicated that the degree of enantioselectivity for chiral recognition system depends on analyte concentration. Thus, 3 concentration levels (0.05, 0.5, and 5.0 mM) of the analyte were designed. As shown in Fig. 3A, the analyte produced visual discernible colors from blue to red, which were dependent on $[Diol]_t$ and *ee* of the analyte, on the chiral AuNPs. Thus the enantioselectivity of the chiral AuNPs could be directly assessed by visual inspection under a moderate concentration level (0.5 mM) of the analyte (Fig. 3A, yellow frame). This was especially helpful to achieve HTS assays because we might rapidly screen out the best chiral AuNPs by the naked eye for an unknown analyte in practical applications.

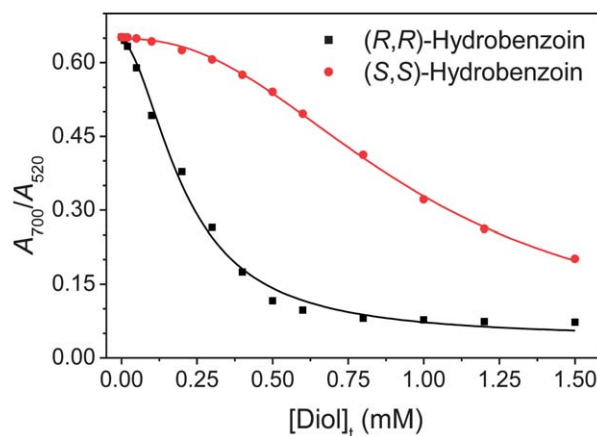


Fig. 2 Enantioselective disassembly titration of *D*-Lac-AuNPs networks with (*R,R*)-hydrobenzoin and (*S,S*)-hydrobenzoin. All titrations were carried out in a mixture of water solutions containing 20 vol% methanol (pH 9.5).

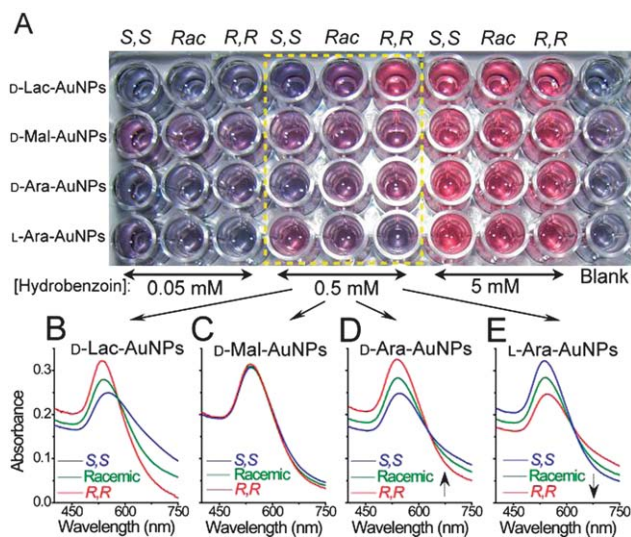


Fig. 3 (A) Image of the enantioselectivity of the screening plate. The distinct colored micro-wells indicated the different response of the chiral AuNPs to the hydrobenzoin with different concentrations (0.05, 0.5, 5.0 mM) of (*R,R*)-hydrobenzoin, (*S,S*)-hydrobenzoin and racemic mixture (Rac as indicated in the image). UV-vis measurements of the screening plate showing enantioselectivity of *D*-Lac-AuNPs (B), *D*-Mal-AuNPs (C), *D*-Ara-AuNPs (D), and *L*-Ara-AuNPs (E) with (*R,R*)-hydrobenzoin (0.5 mM), racemic mixture (0.5 mM) and (*S,S*)-hydrobenzoin (0.5 mM). All the measurements were performed in the mixture of water solutions containing 20 vol% methanol (pH 9.5).

Of the designed chiral AuNPs, *D*-Lac-AuNPs showed the highest enantioselectivity (Fig. 3B–E) and *D*-Mal-AuNPs did not show apparent enantioselectivity (Fig. 3C). Both *D*-Ara- and *L*-Ara-AuNPs showed moderate discrimination between the two enantiomers of hydrobenzoin.

Significantly, the opposite enantiomer-modified chiral AuNPs (*D*-Ara- and *L*-Ara-AuNPs) showed equal and opposite enantioselectivity, which was indicated by the opposite transition of color (Fig. 3A) and the opposite variation of UV-vis spectra (Fig. 3D and E). This result was in good accordance with the first principle of stereochemistry,¹⁷ and indicated the robustness of our method.

Given these results, the screening plate was further quantitatively analyzed with a microplate reader by monitoring the absorbance at 700 and 520 nm. As expected, 96-well plate analysis showed that the two enantiomers of hydrobenzoin were highly enantiodiscriminated by *D*-Lac-AuNPs. An enantioselectivity (defined as $(A_{700}/A_{520})_{SS}/(A_{700}/A_{520})_{RR}$) in the AuNPs signal (A_{700}/A_{520}) ratio of 4.77 was determined with *D*-Lac-AuNPs at 0.5 mM analyte. The enantioselectivity of each chiral AuNPs was listed in Table S1.† Briefly, the results of microplate analysis and visual inspection suggested the same enantioselectivity order of the chiral AuNPs: *D*-Lac-AuNPs > *D*-Ara-AuNPs = *L*-Ara-AuNPs > *D*-Mal-AuNPs, thereby validating the reliability of the screening process.

To display the generality of our method, the enantioselectivity of the chiral AuNPs to two other chiral diols (diethyl tartrate and 1-phenylpropane-1,2-diol) was investigated. As shown in Table S2,† both pairs of enantiomers were successfully enantioselectively recognized. *D*-Mal-AuNPs and *D*-Lac-AuNPs showed the

best enantioselectivity to diethyl tartrate and 1-phenylpropane-1,2-diol, respectively. The results indicated that a different chiral diol might show good response with a different chiral AuNPs, which could be easily screened out from the “chiral AuNPs library” with a screening plate as described above.

The enantioselectivity of the chiral AuNPs was further confirmed by ¹H NMR spectroscopy. As shown in Fig. S8 (ESI†), clear enantio-splitting of the proton NMR signals of the hydrobenzoin methines was monitored in *D*-Lac-AuNPs-borate ion system. The rather large enantiomeric difference in chemical shifts (up to 0.05 ppm) robustly verified the existence of enantioselectivity of *D*-Lac-AuNPs to the two enantiomers of hydrobenzoin. Generally, splitting of the NMR signals of the enantiomers derives from the formation of energetic different diastereomers between the chiral selector and enantiomers.²¹ Thus the NMR results could further indicate the eLE process-based formation of the ternary spiroborates diastereomers (*D*-Lac-borate-hydrobenzoin). The enantio-splitting of the proton NMR signals of the hydrobenzoin methines in *D*-Ara-AuNPs systems was also observed (Fig. S9, ESI†).

Based on the results from the screening plate, the ability of the best *D*-Lac-AuNPs to simultaneously determine $[Diol]_t$ and ee was explored. For this purpose, a “standard plate” with chiral *D*-Lac-AuNPs (Fig. 4, columns 1–11) and achiral DA-AuNPs were made (Fig. 4, column 12). The standard ee titrations of hydrobenzoin were carried out at 6 different $[Diol]_t$ (0.1, 0.2, 0.4, 0.6, 0.8, and 1.0 mM) and 11 different (*R,R*)-hydrobenzoin ee values (–100, –80, –60, –40, –20, 0, 20, 40, 60, 80, and 100)% with *D*-Lac-AuNPs. The standard total concentration ($[Diol]_t$) titration of hydrobenzoin was carried out at 6 different concentrations (0.1, 0.2, 0.4, 0.6, 0.8, and 1.0 mM) with DA-AuNPs. Because DA-AuNP was achiral, it responded only to the change in $[Diol]_t$ of the analyte, whereas *D*-Lac-AuNPs responded to both the change in $[Diol]_t$ and ee of the analyte.

The A_{700}/A_{520} signals of each micro-wells of the standard plate were recorded by a plate reader for the $[Diol]_t$ and ee values of hydrobenzoin as described above were shown in Fig. 5. As commonly adopted in the previous chiral assays,²² the A_{700}/A_{520} values from ee and $[Diol]_t$ titrations were linearly fitted against

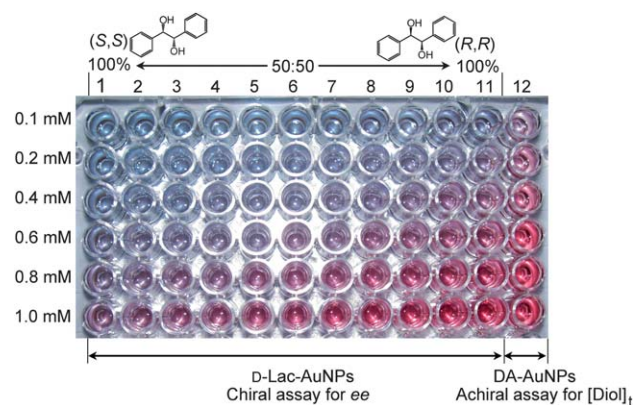


Fig. 4 Layout of the standard plate. Solvent: water–methanol mixture (80 : 20, v/v), pH 9.5. The (*R,R*)-hydrobenzoin ee values of column 1–11 were (–100, –80, –60, –40, –20, 0, 20, 40, 60, 80, 100)%, respectively.

ee and $[\text{Diol}]_t$, respectively. The fitting results were satisfying (correlation coefficients $R^2 > 0.99$).

With the above results, the ability of our method for HTS assay of unknown samples for $[\text{Diol}]_t$ and ee was investigated. To do this, an “analysis plate” was made where the unknown samples with varying $[\text{Diol}]_t$ and ee were tested. By monitoring the A_{700}/A_{520} values, the $[\text{Diol}]_t$ and ee values were predicted according to the standard equations generated from the standard plate (Table S3†). The error for the unknown samples was calculated in the form of average error was determined to be ± 0.05 mM for $[\text{Diol}]_t$ and $\pm 2.72\%$ for ee . The ee correlation graph between the determined values and the actual values had a regression (R^2) of 0.9961, indicating good accuracy (Fig. S10, ESI†).

Overall, the method is rapid once a standard plate has been developed for a particular analyte. Among all the procedures, loading of the AuNPs and unknown sample solutions to the 96-well plate requires about 30 min per 96 samples. After that, the $[\text{Diol}]_t$ and ee values of 96 unknown samples can be predicted within 10 min, including ≈ 5 min for the 96-well plate reader to record the absorbance of 96 unknowns samples at two wavelengths (520 and 700 nm), and 5 min for data analysis with a computer program.

The final performance of this method was evaluated with real samples produced from catalytic AD reactions. The AD reactions generally involve a chiral ligand which plays crucial role in reaction yield and enantioselectivity of its chiral diol products.¹³ A method which can be used for the rapid assay of the reaction yield and ee of AD reactions is highly desired in the

Table 1 Determination of reaction yields and ee values of the four catalytic AD reactions by our HTS and the CE standard methods

Ligands	Time (h)	Yield ^a (%)		ee^b (%)	
		HTS	CE	HTS	CE
(DHQD) ₂ PHAL	7	81.6	80.4	81.4	85.7
(DHQD) ₂ PHAL	15	87.5	86.2	92.8	96.7
(DHQ) ₂ PHAL	7	80.1	78.9	-88.2	-83.8
(DHQ) ₂ PHAL	15	90.7	89.2	-92.4	-96.2

^a The reaction yields were calculated from $[\text{Diol}]_t$. ^b (*R,R*)-hydrobenzoin ee values.

discovery of more efficient chiral ligands. Two commercially available chiral ligands, hydroquinidine 1,4-phthalazinediyl diether (DHQD)₂PHAL and hydroquinine 1,4-phthalazinediyl diether (DHQ)₂PHAL were examined. The literature reported that catalytic AD of *trans*-stilbene with (DHQD)₂PHAL and (DHQ)₂PHAL formed (*R,R*)- and (*S,S*)-hydrobenzoin with highly enantiopurity, respectively.^{13,23}

AD reactions of *trans*-stilbene with the two chiral ligands were performed according to the literature procedures.²³ Analysis of the crude reaction products was carried in two steps: the reaction yield was firstly identified through the determination of $[\text{Diol}]_t$ on a DA-AuNPs generated “analysis plate”; and according to determined $[\text{Diol}]_t$, another “analysis plate” was generated with D-Lac-AuNPs for the assay of ee values. Although such a “two step” assay was already high-throughput and rapid, the assay could be further improved on a single “analysis plate” with the help of Statistica Neural Network software as reported by Anslyn's group.¹⁷

Four AD reactions of *trans*-stilbene were carried out with different reaction time (7 and 15 h) and chiral ligands ((DHQD)₂PHAL and (DHQ)₂PHAL). The reaction yield and ee values predicted by our HTS method and the standard CE method¹² were listed in Table 1. Apparently, the results of the HTS method compared favorably with those from the standard CE,¹² indicating that the co-reactants of the AD reactions did not interfere with the determination accuracy of our HTS method. Presumably, using this method, dozens to hundreds of AD reactions could be simultaneously analyzed in a few minutes. However, a single CE separation of hydrobenzoin enantiomers requires much longer time (Fig. S11, ESI†). We also found that the sample solutions displayed different colors in the range from blue to red as the yield and ee varied. This allowed us to semi-quantitatively screening the AD reactions with the naked eye.

Conclusions

On the basis of the reversibility of boron chemistry and the plasmon resonance character of AuNPs, we demonstrate, for the first time, that spiroborate cross-linked AuNP hybrids show highly enantioselectivity and can be a HTS assay of ee and $[\text{Diol}]_t$ of chiral vicinal diols. The underlying enantiorecognition events have been further confirmed by NMR spectroscopy, and the method has been successfully used to rapidly analyze real AD

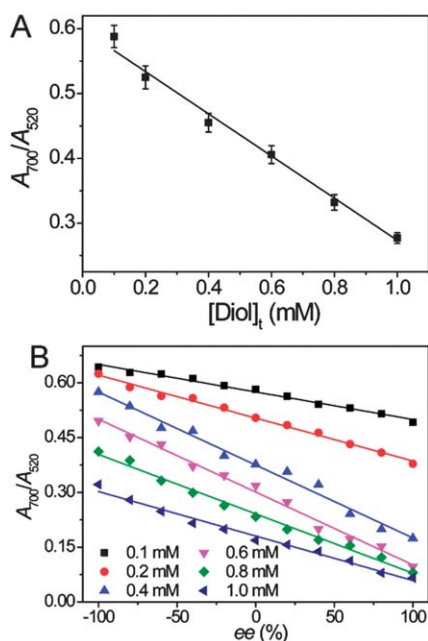


Fig. 5 Analysis of the standard plate. (A) $[\text{Diol}]_t$ titration of DA-AuNPs at 6 different concentrations of racemic hydrobenzoin. (B) (*R,R*)-hydrobenzoin ee titration of D-Lac-AuNPs (0.04 mM surface bound D-Lac with 0.02 mM borate ion) at 6 different $[\text{Diol}]_t$: 0.1 (■), 0.2 (●), 0.4 (▲), 0.6 (▼), 0.8 (◆), and 1.0 mM (◄). All samples were made in the mixture of water solutions containing 20 vol% methanol (pH 9.5).

reactions of *trans*-stilbene with different reaction time and chiral ligands. Since this proof of concept approach is based on enantioselective ligand exchange principle and the reversibility of boron chemistry, it can be easily adapted to other kinds of asymmetric reactions by using relevant optical nanoprobe. On the other hand, chiral selective assembly of nanoparticles could also be achieved in other manners by modifying with different chiral molecules.²⁴

Experimental section

Materials

Gold(III) chloride trihydrate (HAuCl₄), trisodium citrate dihydrate (citrate), thioctic acid, boric acid, D-lactose, D-maltose, were purchased from Sigma Aldrich (St. Louis, MO). D-Arabinose, L-arabinose, (*R,R*)-hydrobenzoin, (*S,S*)-hydrobenzoin, diethyl D-tartrate, diethyl L-tartrate, (1*R*,2*R*)-1-phenylpropane-1,2-diol, and (1*S*,2*S*)-1-phenylpropane-1,2-diol were purchased from Fisher Scientific (Pittsburgh, PA). 1-Ethyl-3(3-dimethylaminopropyl) carbodiimide hydrochloride (EDC·HCl), and *N*-hydroxysuccinimide (NHS) were purchased from Alfa Aesar (Ward Hill, MA). Dialysis membrane was purchased from Pierce (3000 MWCO). All other reagents were of analytical reagent grade. Ultra-pure water (18.2 MΩ cm⁻¹, Milli-Q, Millipore) was used for all experiments.

Instrumentation

Ultraviolet-visible spectroscopy (UV-vis) measurements were recorded on a Jasco-V550 UV-vis spectrophotometer. Fourier transform infrared spectroscopy (FTIR) measurements were carried out with a BRUKER Vertex 70 FTIR spectrometer. The sample was prepared as pellets using spectroscopic grade KBr. Transmission electron microscopic (TEM) experiments were performed using a Philips Tacnai G2 20 S-TWIN microscope operating at 200 kV. For visualization by TEM, samples were prepared by dropping a solution of production on a copper grid. The dynamic light scattering (DLS) measurements were carried out using a Zeta PALS analyzer (Brookhaven Instruments Corp. Holtsville, NY). ¹H nuclear magnetic resonance (NMR) spectra were recorded at 25 °C on a Bruker Avance 600 MHz NMR Spectrometer. X-ray photoelectron spectroscopy (XPS) data were obtained with an ESCALab220i-XL electron spectrometer from VG Scientific using 300 W AlK α radiation. The base pressure was about 3 × 10⁻⁹ mbar. The binding energies were referenced to the C 1s line at 284.8 eV from adventitious carbon. Curve fitting was performed using a Gaussian–Lorentzian peak shape.

The 96-well plate analysis

Arrays were made by mixing AuNPs, borate ion, and analyte stock solutions within Corning 96-well polystyrene plates. Absorbance spectra were recorded at ambient temperature on a Bio-Gen Technology PHERAstar FS multidetection microplate reader. Each well contained a total solution volume of 300 μL. After making the plate, it was sealed to prevent solvent evaporation. All samples were equilibrated for at least 10 min before measurements. All measurements were taken at 25 °C.

A “screening plate” was designed at 3 different analyte (hydrobenzoin) concentrations 0.05, 0.50, 5.00 mM, and the each chiral AuNP and borate ions (surface-bound diols : borate = 2 : 1 equiv.) were added to each well of the microplate. The establishment of standard equations for *ee* and total concentration ([Diol]_t) was combined on a “standard plate” to speed up the analysis. The standard plate was designed with D-Lac-AuNPs (chiral assays for *ee*) and DA-AuNPs (achiral assays for [Diol]_t). The layout for the standard plate was such that the concentration of the analyte (hydrobenzoin) would vary along each row of the plate, whereas the *ee* of the solution varied from 100% to –100% (column 1–11) and column 12 was racemic hydrobenzoin for achiral assay (Fig. 4). The “analysis plates” were prepared for sample analysis, and the amount of chiral/achiral AuNPs and borate (including other conditions) were the same to the standard plate.

Acknowledgements

This work was supported by 973 Project (2011CB936004, 2012CB720602), NSFC (20831003, 91213302, 20833006, 21210002), and Funds from the Chinese Academy of Sciences.

Notes and references

- (a) S. J. Rowan, S. J. Cantrill, G. R. L. Cousins, J. K. M. Sanders and J. F. Stoddart, *Angew. Chem., Int. Ed.*, 2002, **41**, 898–952; (b) R. Nishiyabu, Y. Kubo, T. D. James and J. S. Fossey, *Chem. Commun.*, 2011, **47**, 1124–1150; (c) R. Nishiyabu, Y. Kubo, T. D. James and J. S. Fossey, *Chem. Commun.*, 2011, **47**, 1106–1123.
- (a) A. Deutsch and S. Osoling, *J. Am. Chem. Soc.*, 1949, **71**, 1637–1640; (b) E. W. Malcolm, *A Study of the Borate-Carbohydrate Complex Formed in an Aqueous Medium*, Appleton, Wisconsin, 1964; (c) A. P. Bapat, D. Roy, J. G. Ray, D. A. Savin and B. S. Sumerlin, *J. Am. Chem. Soc.*, 2011, **133**, 19832–19838.
- J. A. Riggs, R. K. Litchfield and B. D. Smith, *J. Org. Chem.*, 1996, **61**, 1148–1150.
- R. Mathur, S. Bohra, V. Mathur, C. Narang and N. Mathur, *Chromatographia*, 1992, **33**, 336–338.
- (a) P. D. Beer and P. A. Gale, *Angew. Chem., Int. Ed.*, 2001, **40**, 486–516; (b) N. Kameta and K. Hiratani, *Tetrahedron Lett.*, 2006, **47**, 4947–4950; (c) N. Kameta and K. Hiratani, *Chem. Commun.*, 2005, 725–727.
- (a) S. Gao, J. Guo and K. Nishinari, *Carbohydr. Polym.*, 2008, **72**, 315–325; (b) E. Pezron, A. Ricard, F. Lafuma and R. Audebert, *Macromolecules*, 1988, **21**, 1121–1125.
- (a) M. A. O'Neill, S. Eberhard, P. Albersheim and A. G. Darvill, *Science*, 2001, **294**, 846–849; (b) T. L. Holdaway-Clarke, N. M. Weddle, S. Kim, A. Robi, C. Parris, J. G. Kunkel and P. K. Hepler, *J. Exp. Bot.*, 2003, **54**, 65–72.
- S. Tamesue, M. Numata, K. Kaneko, T. D. James and S. Shinkai, *Chem. Commun.*, 2008, 4478–4480.
- (a) Y. Liu, X. Han, L. He and Y. Yin, *Angew. Chem., Int. Ed.*, 2012, **51**, 6373–6377; (b) M.-C. Daniel and D. Astruc, *Chem. Rev.*, 2004, **104**, 293–346.

- 10 (a) S. Kodama, A. Yamamoto, R. Iio, K. Sakamoto, A. Matsunaga and K. Hayakawa, *Analyst*, 2004, **129**, 1238–1242; (b) S. Kodama, S. Aizawa, A. Taga, T. Yamashita and A. Yamamoto, *Electrophoresis*, 2006, **27**, 4730–4734; (c) S. Kodama, S.-I. Aizawa, A. Taga, T. Yamashita, T. Kemmei, A. Yamamoto and K. Hayakawa, *Electrophoresis*, 2007, **28**, 3930–3933; (d) M. G. Schmid, N. Grobuschek, O. Lecnik and G. J. Gübitz, *J. Biochem. Biophys. Methods*, 2001, **48**, 143–154.
- 11 J. A. Raskatov, J. M. Brown and A. L. Thompson, *CrystEngComm*, 2011, **13**, 2923–2929.
- 12 P. Liu, W. He, Y. Zhao, P.-A. Wang, X.-L. Sun, X.-Y. Li and S.-Y. Zhang, *Chirality*, 2008, **20**, 75–83.
- 13 H. C. Kolb, M. S. VanNieuwenhze and K. B. Sharpless, *Chem. Rev.*, 1994, **94**, 2483–2547.
- 14 A. M. Kelly, Y. Pérez-Fuertes, J. S. Fossey, S. L. Yeste, S. D. Bull and T. D. James, *Nat. Protoc.*, 2008, **3**, 215–219.
- 15 (a) T. Ishii and H. Ono, *Carbohydr. Res.*, 1999, **321**, 257–260; (b) J. A. Riggs, R. K. Litchfield and B. D. Smith, *J. Org. Chem.*, 1996, **61**, 1148–1150; (c) P. Britz-McKibbin and D. D. Y. Chen, *Anal. Chem.*, 2000, **72**, 1242–1252; (d) R. A. Wallingford and A. G. Ewing, *Anal. Chem.*, 1989, **61**, 98–100.
- 16 (a) S.-Y. Lin, Y.-T. Tsai, C.-C. Chen, C.-M. Lin and C.-H. Chen, *J. Phys. Chem. B*, 2004, **108**, 2134–2139; (b) J. M. Abad, S. F. L. Mertens, M. Pita, V. M. Fernández and D. J. Schiffrin, *J. Am. Chem. Soc.*, 2005, **127**, 5689–5694.
- 17 (a) S. H. Shabbir, C. J. Regan and E. V. Anslyn, *Proc. Natl. Acad. Sci. U. S. A.*, 2009, **106**, 10487–10492; (b) S. H. Shabbir, L. A. Joyce, G. M. da Cruz, V. M. Lynch, S. Sorey and E. V. Anslyn, *J. Am. Chem. Soc.*, 2009, **131**, 13125–13131.
- 18 S. Xing, Y. Guan and Y. Zhang, *Macromolecules*, 2011, **44**, 4479–4436.
- 19 (a) J. Wang, L. Wu, J. Ren and X. Qu, *Small*, 2012, **8**, 259–264; (b) D. Li, A. Wiecekowska and I. Willner, *Angew. Chem., Int. Ed.*, 2008, **47**, 3927–3931; (c) X. Xie, W. Xu and X. Liu, *Acc. Chem. Res.*, 2012, **45**, 1511–1520.
- 20 (a) W. Wei, K. Qu, J. Ren and X. Qu, *Chem. Sci.*, 2011, **2**, 2050–2056; (b) W. Wei, B.-Y. Guo and J.-M. Lin, *J. Chromatogr., A*, 2009, **1216**, 1484–1489; (c) W. Wei, B. Guo and J.-M. Lin, *Electrophoresis*, 2009, **30**, 1380–1387.
- 21 (a) C. Naumann, W. A. Bubba, B. E. Chapman and P. W. Kuchel, *J. Am. Chem. Soc.*, 2007, **129**, 5340–5341; (b) G. Uccello-Barretta, F. Balzano, R. Menicagli and P. Salvadori, *J. Org. Chem.*, 1996, **61**, 363–365.
- 22 (a) G. Mirri, S. D. Bull, P. N. Horton, T. D. James, L. Male and J. H. R. Tucker, *J. Am. Chem. Soc.*, 2010, **132**, 8903–8905; (b) J. F. Folmer-Andersen, V. M. Lynch and E. V. Anslyn, *J. Am. Chem. Soc.*, 2005, **127**, 7986–7987; (c) X. F. Mei and C. Wolf, *J. Am. Chem. Soc.*, 2006, **128**, 13326–13327.
- 23 (a) E. N. Jacobsen, I. Marko, W. S. Mungall, G. Schroder and K. B. Sharpless, *J. Am. Chem. Soc.*, 1988, **110**, 1968–1970; (b) T. P. Yoon and E. N. Jacobsen, *Science*, 2003, **299**, 1691–1693.
- 24 D. Balogh, Z. Zhang, A. Ceconello, J. Vavra, L. Severa, F. Teply and I. Willner, *Nano Lett.*, 2012, **12**, 5835–5839.